New La$_2$CuO$_4$ Derivatives La$_{2-2x}$Sr$_{2x}$Cu$_{1-x}$M$_x$O$_4$ (M=Ti, Mn, Fe, or Ru): A Study of Linear Cu–O–M Electronic Interaction in Two Dimensions[1]

K. Ramesha, S. Uma, N. Y. Vasanthacharya, and J. Gopalakrishnan[2]

Solid State and Structural Chemistry Unit, Indian Institute of Science, Bangalore 560 012, India

Oxides of the general formula La$_{2-2x}$Sr$_{2x}$Cu$^{II}_{1-x}$M$^{IV}_x$O$_4$ (M = Ti, Mn, Fe, or Ru), crystallizing in the tetragonal K$_2$NiF$_4$ structure, have been synthesized. For *M*=Ti, only the *x*=0.5 member could be prepared, while for *M*=Mn and Fe, the composition range is 0<*x*<1.0, and for *M*=Ru, the composition range is 0<*x* ≤ 0.5. There is no evidence for an ordering of Cu(II) and *M*(IV) in the *x*=0.5 members. While the members of the *M*=Ti, Mn, and Ru series are semiconducting/insulating, the members of the *M*=Fe series are metallic, showing a broad metal–semiconductor transition around 100 K for 0<*x* ≤ 0.15 that is possibly related to a Cu(II)–O–Fe(IV)↔Cu(III)–O–Fe(III) valence degeneracy. Increasing the strontium content at the expense of lanthanum in La$_{2-2x}$Sr$_{2x}$Cu$_{1-x}$Fe$_x$O$_4$ for *x* ≤ 0.20 renders the samples metallic but not superconducting. © 1997 Academic Press

INTRODUCTION

After the discovery of high Tc superconductivity in the alkaline-earth metal substituted La$_2$CuO$_4$ (1, 2), substitution of a wide variety of metal atoms at the lanthanum and copper sites of both the parent La$_2$CuO$_4$ and superconducting La$_{2-x}$Sr$_x$CuO$_4$ have been investigated (3, 4). Here we report a new kind of substitution in La$_2$CuO$_4$ that involves both the lanthanum and the copper sites, viz., La$_{2-2x}$Sr$_{2x}$Cu$_{1-x}$M$_x$O$_4$, where *M* is a metal such as Ti, Mn, Fe, or Ru that takes quadrivalency. The motivation of this work is two-fold. The first is to find out whether charge-compensated substitution of tetravalent *M* atoms at the copper sites in La$_{2-2x}$Sr$_{2x}$Cu$_{1-x}$M$_x$O$_4$ would produce an ordering of Cu and M atoms. Ordering of Cu(II) and *M*(IV) is known in La$_2$CuMO$_6$ (*M* = Ti, Mn, Sn) perovskites giving rise to novel superstructures (5, 6). The second, more important, motivation is to find out whether the substitution of transition metal *M*(IV) atoms, such as Mn(IV),

Fe(IV), or Ru(IV), in the CuO$_2$ sheets would produce a Cu(II)–O–*M*(IV)↔Cu(III)–O–*M*(III) valence degeneracy. Valence degeneracy between Fe(II)–O–Re(VI) in Ba$_2$FeReO$_6$ and between Fe(II)–O–Mo(VI) in A_2FeMoO$_6$ (A = Ca, Sr, Ba) perovskites gives rise to interesting metallic and ferrimagnetic properties (8). Among the several *M* atoms investigated by us in the La$_{2-2x}$Sr$_{2x}$Cu$_{1-x}$M$_x$O$_4$ series, we find that the members of the *M* = Fe series show a metallic behavior and a broad metal–semiconductor transition at *T* < 100 K in the limited composition range 0 < *x* ≤ 0.15, that is probably related to a Cu(II)–O–Fe(IV)↔Cu(III)–O–Fe(III) valence degeneracy.

EXPERIMENTAL

Samples of La$_{2-2x}$Sr$_{2x}$Cu$_{1-x}$M$_x$O$_4$ for *M* = Ti or Ru were prepared by mixing stoichiometric quantities of high-purity La$_2$O$_3$, SrCO$_3$, CuO, and TiO$_2$ or RuO$_2$ (>99%, purchased from Fluka/Aldrich). Pressed pellets of the oxides were reacted at 1150°C for 48 h with one intermediate grinding. Samples of La$_{2-2x}$Sr$_{2x}$Cu$_{1-x}$M$_x$O$_4$ for *M* = Mn or Fe were synthesized by dissolving stoichiometric proportions of La$_2$O$_3$, SrCO$_3$, and Mn(C$_2$O$_4$)·2H$_2$O or Fe(C$_2$O$_4$)·2H$_2$O in 8 *M* nitric acid. The homogeneous solutions of metal nitrates were dried and slowly decomposed at 600°C for 6 h. The powders were pressed into pellets and sintered at 1150°C for 48 h with intermediate grinding and pelletizing. The oxygen content due to higher oxidation states of the transition metals was determined by iodometric titration using KI (9).

The oxides were characterized by X-ray powder diffraction (XRD) using (JEOL JDX-8P X-ray powder diffractometer, CuKα radiation). Unit cell parameters were derived by least-squares refinement of the powder diffraction data using the PROSZKI program (10). For selected samples, electron diffraction patterns were recorded using a JEOL JEM 200-CX transmission electron microscope.

Electrical resistivity measurements were carried out on sinterd pellets by a four-probe technique in the temperature range 300–15 K using a closed-cycle helium cryostat.

[2] To whom correspondence should be addressed.

DC magnetic susceptibility measurements were made in the 300–15 K range using a Lewis Coil magnetometer (George Associates, Model 2000).

RESULTS AND DISCUSSION

Synthesis and Structural Characterization

Solid solutions corresponding to the composition, $La_{2-2x}Sr_{2x}Cu_{1-x}M_xO_4$, could be readily prepared for $M = Mn$ and Fe ($0 < x < 1.0$) and Ru ($0 < x < 0.5$). For $M = Ti$, only the $x = 0.5$ member, $LaSrCu_{0.5}Ti_{0.5}O_4$, could be prepared. All the products are single-phase materials as revealed by powder XRD, crystallizing in K_2NiF_4-like structures. Typical XRD patterns of a few representative members of $La_{2-2x}Sr_{2x}Cu_{1-x}M_xO_y$ ($M = Ti$, Mn, Ru, and Fe) are shown in Figs. 1 and 2. While the compositions with $x > 0.1$ are tetragonal ($I4/mmm$), presence of an orthorhombic distortion is clearly seen in the members with $x = 0.05$.

Iodometric titration show that the samples are nearly stoichiometric having the expected oxygen content close to 4.0 per formula unit in most of the cases, excepting those with $M = Fe$ for $x \geq 0.25$. This reveals that the solid solutions could be formulated as $La_{2-2x}Sr_{2x}Cu_{1-x}^{II}M_x^{IV}O_4$ for $M = Mn$, Ru, or Ti. For $M = Fe$, this formula holds

good up to $x = 0.20$; for $x \geq 0.25$, the samples are oxygen-deficient indicating that not all the Fe is present in the tetravalent state. Annealing in oxygen at 900 as well as 400°C did not improve the oxygen stoichiometry of Fe containing samples with $x > 0.25$.

The compositions and the refined tetragonal lattice parameters are given in Table 1. We do not see extra reflections (other than those expected for the K_2NiF_4 structure) in the XRD patterns of $La_{2-2x}Sr_{2x}Cu_{1-x}M_xO_y$ ($M = Ti$, Mn, Fe, or Ru) indicating the absence of a superstructure due to long-range ordering of Cu and M atoms. This is further confirmed by electron diffraction (ED) investigations. The $[0\,0\,1]$ and $[1\,0\,0]$ reciprocal sections of $LaSrCu_{0.5}Ti_{0.50}O_4$ (Fig. 3) reveal a tetragonal K_2NiF_4-like structure without any superlattice ordering.

While the variation of lattice parameters of $La_{2-2x}Sr_{2x}Cu_{1-x}M_xO_4$ with x for $M = Mn$ and Ru does not show an obvious anomaly (Table 1), we do find an anomalous behavior for the $M = Fe$ system (Fig. 4). The a parameter decreases with x showing a minimum at $x = 0.15$; for $x > 0.15$, the a parameter increases, while the c parameter and the c/a ratio continuously decrease with x. Considering the lattice parameters of the end members (La_2CuO_4, pseudotetragonal $a = 3.810$ and $c = 13.15$ Å (11); Sr_2FeO_4, $a = 3.863$ and $c = 12.406$ Å (12)), one would have expected a continuous increase of a and decrease of

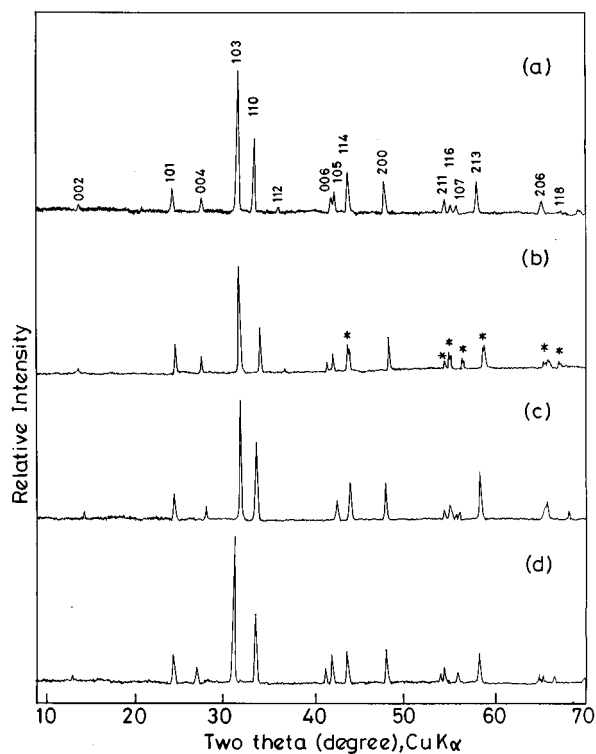FIG. 1. X-ray powder diffraction patterns of (a) $LaSrCu_{0.50}Ti_{0.50}O_4$, (b) $La_{1.90}Sr_{0.10}Cu_{0.95}Mn_{0.05}O_4$, (c) $LaSrCu_{0.50}Mn_{0.50}O_4$, and (d) $La_{1.80}Sr_{0.20}Cu_{0.90}Ru_{0.10}O_4$.
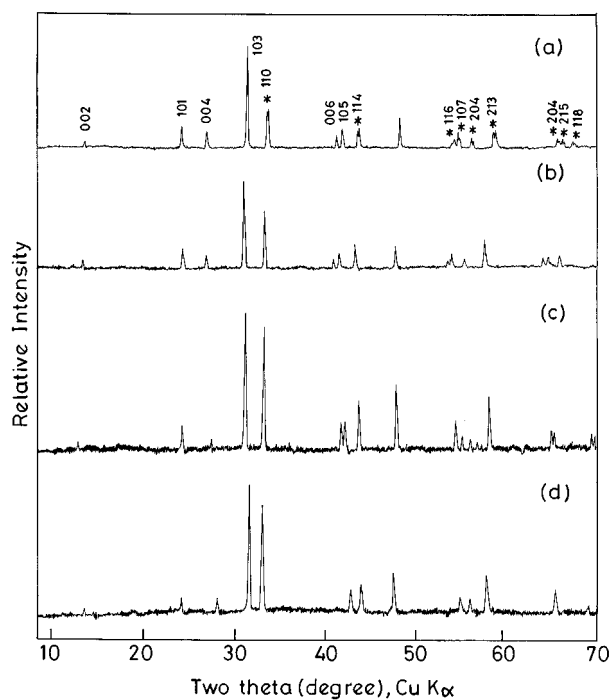

FIG. 2. X-ray powder diffraction patterns of $La_{2-2x}Sr_{2x}Cu_{1-x}$ Fe_xO_{4-y} members: (a) $x = 0.05$, (b) $x = 0.10$, (c) $x = 0.50$, and (d) $x = 0.75$.

TABLE 1
Lattice Parameters and Oxygen Contents of La$_{2-2x}$Sr$_{2x}$Cu$_{1-x}$M$_x$O$_y$ (M = Mn, Ru, Fe) Members

| Compound | Lattice parameters (Å) | | Oxygen content[a] |
	a	c	y
La$_{1.90}$Sr$_{0.10}$Cu$_{0.95}$Mn$_{0.05}$O$_y$[b]	3.794(1)	13.146(4)	4.00
La$_{1.80}$Sr$_{0.20}$Cu$_{0.90}$Mn$_{0.10}$O$_y$	3.793(1)	13.139(4)	4.01
LaSrCu$_{0.50}$Mn$_{0.50}$O$_y$	3.807(1)	12.745(1)	3.99
La$_{1.90}$Sr$_{0.10}$Cu$_{0.95}$Ru$_{0.05}$O$_y$[b]	3.794(1)	13.179(5)	4.00
La$_{1.80}$Sr$_{0.20}$Cu$_{0.90}$Ru$_{0.10}$O$_y$	3.795(1)	13.175(3)	3.99
LaSrCu$_{0.50}$Ti$_{0.50}$O$_y$	3.818(1)	13.003(5)	4.00
La$_{1.90}$Sr$_{0.10}$Cu$_{0.95}$Fe$_{0.05}$O$_y$[b]	3.795(1)	13.164(5)	4.00
La$_{1.80}$Sr$_{0.20}$Cu$_{0.90}$Fe$_{0.10}$O$_y$	3.787(1)	13.173(5)	4.00
La$_{1.70}$Sr$_{0.30}$Cu$_{0.85}$Fe$_{0.15}$O$_y$	3.782(1)	13.169(4)	4.00
La$_{1.60}$Sr$_{0.40}$Cu$_{0.80}$Fe$_{0.20}$O$_y$	3.784(1)	13.168(4)	4.00
La$_{1.50}$Sr$_{0.50}$Cu$_{0.75}$Fe$_{0.25}$O$_y$	3.786(1)	13.166(3)	3.94
LaSrCu$_{0.50}$Fe$_{0.50}$O$_y$	3.802(1)	12.956(3)	3.90
La$_{0.50}$Sr$_{1.50}$Cu$_{0.25}$Fe$_{0.75}$O$_y$	3.832(1)	12.678(5)	3.80

[a] Determined by iodometric titration.
[b] Pseudotetragonal cell parameters are given here. The real cell is most likely orthorhombic.

c with x across the series La$_{2-2x}$Sr$_{2x}$Cu$_{1-x}$Fe$_x$O$_4$. The anomalous variation of lattice parameters signals a complex behavior presumably arising from the electronic configuration of Fe(IV). We shall offer an explanation for the anomalous variation of lattice parameters together with the electrical and magnetic properties of M = Fe system in the next section.

Electrical and Magnetic Properties

The electrical and magnetic properties of La$_{2-2x}$Sr$_{2x}$Cu$_{1-x}$M$_x$O$_4$ members show an interesting variation that reflects the effect of aliovalent M(IV) cation substitution at the Cu sites of La$_2$CuO$_4$. The x = 0.5 member of M = Ti phase, LaSrCu$_{0.5}$Ti$_{0.5}$O$_4$, shows the expected semiconducting ($\rho_{300K} \sim 6.5 \times 10^2$ ohm/cm) and paramagnetic behavior which is understandable in terms of random substitution of diamagnetic Ti(IV): $3d^0$ cations at the Cu(II): $3d^9$ sites in La$_2$CuO$_4$. The temperature variation of the susceptibility (Fig. 5) after correcting for core diamagnetism (13) is Curie–Weiss-like below 220 K; the χ_M^{-1} versus T plot shows a small positive curvature at $T > 220$ K. The experimental Curie constants, C_M, 0.058 at $T < 220$ K and 0.045 at $T > 220$ K, are considerably smaller than the ideal value (0.187) expected for isolated Cu(II): $3d^9$ configuration. The low moments are consistent with a random distribution of Cu(II) and Ti(IV) atoms at the octahedral sites of La$_2$CuO$_4$/K$_2$NiF$_4$ structure, which would give rise to a finite fraction of Cu–O–Cu interactions. It is noteworthy that the magnetic behavior of
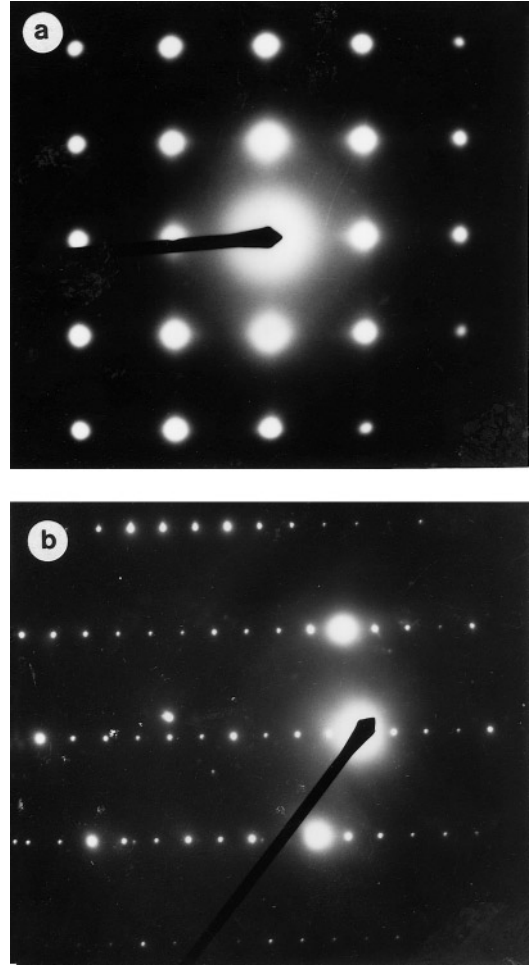
FIG. 3. Electron diffraction patterns of LaSrCu$_{0.50}$Ti$_{0.50}$O$_4$. Zone axes are (a) (0 0 1) and (b) (1 0 0).

LaSrCu$_{0.5}$Ti$_{0.5}$O$_4$ is different from that of La$_2$CuTiO$_6$ (14) and La$_2$Ba$_2$Cu$_2$Ti$_2$O$_{11-\delta}$ (15) in that the χ_M^{-1} versus T plots of the latter oxides show a negative curvature at low temperatures.

The electrical resistivity (ρ) behavior of La$_{2-2x}$Sr$_{2x}$Cu$_{1-x}$M$_x$O$_4$ for M = Mn(IV) and Ru(IV) is similar; ρ increases with x indicating that the charge carriers are increasingly localized. The activation energy (E_a) derived from log ρ versus T^{-1} plots (Fig. 6) also increases with x (Table 2). The results reveal that Cu(II)–O–M(IV)–O–Cu(II) (M = Mn, Ru) interactions are insulating in nature for both Mn(IV) and Ru(IV) in the sense that they do not permit an itinerant electron transport. The results reveal that charge-coupled substitution of Mn(IV) and Ru(IV) at Cu(II) sites in La$_2$CuO$_4$ localizes the charge carriers and that the Cu(II)–O–M(IV) interactions in La$_{2-2x}$Sr$_{2x}$Cu$_{1-x}$M$_x$O$_4$ (M = Mn, Ru) do not permit an itinerant electron transport.
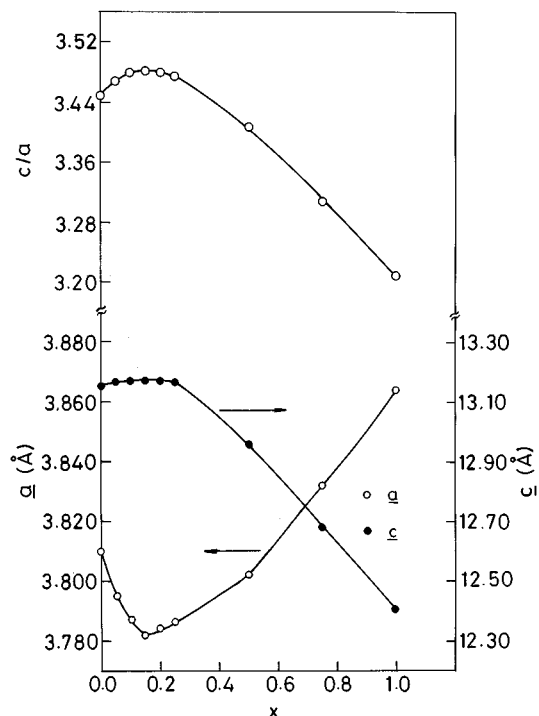
FIG. 4. Variation of the unit cell parameters (a, c) and c/a ratio of $La_{2-2x}Sr_{2x}Cu_{1-x}Fe_xO_{4-y}$ with x.

Interestingly, the electrical resistivity behavior of the $La_{2-2x}Sr_{2x}Cu_{1-x}Fe_xO_4$ system is different. For $x \leq 0.15$, the resistivity decreases and for $x > 0.15$, it increases with x. The temperature dependence of the resistivity (Fig. 7) shows that the samples are metallic for $T > 100$ K; at lower temperatures, there is an upturn of the resistivity plot indicating a metal–semiconductor transition that occurs over a wide temperature range. The sample with $x = 0.15$ shows the lowest resistivity and its temperature dependence is metallic
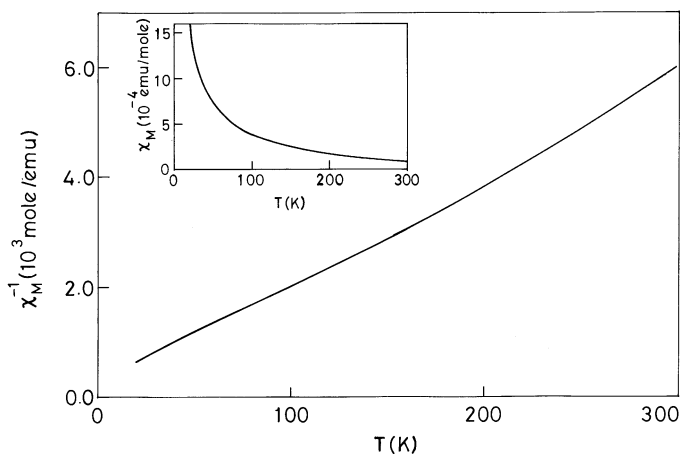

FIG. 6. Plots of log resistivity ($\log \rho$) versus inverse temperature (T^{-1}) for $La_{2-2x}Sr_{2x}Cu_{1-x}M_xO_4$ ($M = $ Mn, Ru). (a) $M = $ Ru; $x = 0.05$, (b) $M = $ Mn; $x = 0.05$, (c) $M = $ Ru; $x = 0.10$, and (d) $M = $ Mn; $x = 0.10$. Inset shows the corresponding data for $M = $ Mn; $x = 0.50$.

for $T > 80$ K. For $T < 80$ K, this sample also shows a slight upturn in the resistivity curve indicating the tendency toward semiconducting behavior. Clearly the Fe(IV)–O–Cu(II) interaction in this composition range is itinerant. There is a striking correlation between the lattice parameter variation (Fig. 4) and electrical resistivity behavior in this system. Thus, there is a decrease in the a parameter which parallels the decrease in resistivity with x up to 0.15; the $x = 0.15$ sample which shows the lowest resistivity also has the smallest a parameter (3.782 Å).

It is most likely that both the variation of lattice parameters and the electrical resistivity of $La_{2-2x}Sr_{2x}$

FIG. 5. Plot of inverse molar magnetic susceptibility (χ_M^{-1}) versus temperature (T) for $LaSrCu_{0.50}Ti_{0.50}O_4$. Inset shows the corresponding χ_M versus T plot.
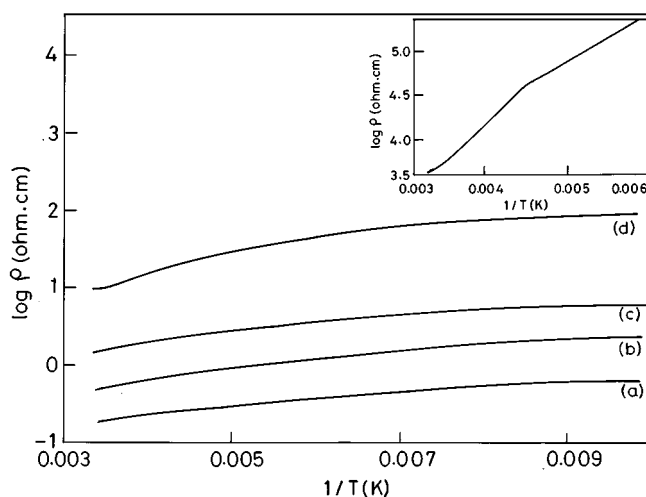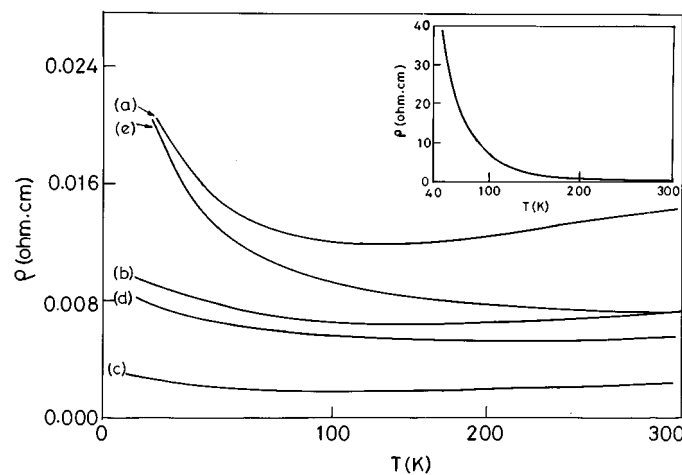

FIG. 7. Plots of resistivity (ρ) versus temperature (T) for $La_{2-2x}Sr_{2x}Cu_{1-x}Fe_xO_4$. (a) $x = 0.05$, (b) $x = 0.10$, (c) $x = 0.15$, (d) $x = 0.20$, and (e) $x = 0.25$. Inset shows the corresponding data for $x = 0.50$.

TABLE 2
Electrical Resistivity and Magnetic Susceptibility Data for La$_{2-2x}$Sr$_{2x}$Cu$_{1-x}$M$_x$O$_y$ (M = Ti, Mn, Ru, Fe) Members

Compound	ρ_{300K} (ohm.cm)	E_a (eV)	C_M (exp) (emu.K/mole)	C_M (calc) (emu.K/mole)
LaSrCu$_{0.50}$Ti$_{0.50}$O$_4$	6.50×10^2	0.12	0.045 (300–220 K)	0.187
			0.058 (220–20 K)	
La$_{1.90}$Sr$_{0.10}$Cu$_{0.95}$Mn$_{0.05}$O$_4$	5.00×10^{-1}	0.02		
La$_{1.80}$Sr$_{0.20}$Cu$_{0.90}$Mn$_{0.10}$O$_4$	1.00×10^1	0.05		
LaSrCu$_{0.50}$Mn$_{0.50}$O$_4$	4.40×10^3	0.18	1.18 (300–100 K)	1.125
La$_{1.90}$Sr$_{0.10}$Cu$_{0.95}$Ru$_{0.05}$O$_4$	1.90×10^{-1}	0.02		
La$_{1.80}$Sr$_{0.20}$Cu$_{0.90}$Ru$_{0.10}$O$_4$	0.15×10^1	0.03		
LaSrCu$_{0.50}$Ru$_{0.50}$O$_4$	1.00×10^2	0.13		
La$_{1.90}$Sr$_{0.10}$Cu$_{0.95}$Fe$_{0.05}$O$_4$	1.40×10^{-2}	Metallic		
La$_{1.70}$Sr$_{0.30}$Cu$_{0.85}$Fe$_{0.15}$O$_4$	2.30×10^{-3}	Metallic	0.49 (300–120 K)	0.77
			0.35 (120–20 K)	
La$_{1.60}$Sr$_{0.40}$Cu$_{0.80}$Fe$_{0.20}$O$_4$	5.50×10^{-3}	0.002		
LaSrCu$_{0.50}$Fe$_{0.50}$O$_{3.9}$	2.70×10^{-1}	0.05	1.58 (300–200 K)	1.68

Cu$_{1-x}$Fe$_x$O$_4$ have their origin in the electronic structure/configuration of Fe. Chemical titrations (Table 1) show that there is no oxygen nonstoichiometry for $x \leq 0.20$. This result is consistent with either Cu(II) + Fe(IV) or Cu(III) + Fe(III) valence states. We believe that the former valence combination is more likely because of the itinerant electron conduction of the samples in this composition range.

Fe(IV): $3d^4$ in perovskite and related oxides has been known to show a rich variety of electronic configurations giving rise to a diversity of electrical and magnetic properties. For example, Fe(IV) has the high-spin configuration $t_{2g}^3\sigma^{*1}$ (localized t_{2g} and itinerant e_g electrons) in SrFeO$_3$ that makes it antiferromagnetic ($T_N = 134$ K) and metallic down to 4 K (16). CaFeO$_3$, on the other hand, is antiferromagnetic ($T_N = 116$ K) and insulating, and these properties have been attributed to the valence disproportion, $2\text{Fe(IV)} (t_{2g}^3\sigma^{*1}) \rightleftharpoons \text{Fe(III)} (t_{2g}^3 e_g^2) + \text{Fe(V)}(t_{2g}^3)$ (17). Fe(IV) in Sr$_2$FeO$_4$ has been assigned the high-spin $t_{2g}^3 e_g^1$ configuration (localized t_{2g} and e_g electrons) that is consistent with its antiferromagnetic ($T_N = 60$ K) and insulating properties (12). In both SrFeO$_3$ and Sr$_2$FeO$_4$, the high-spin Fe(IV): $3d^4$ configuration appears to be heavily admixed with the O $2p \rightarrow$ Fe $3d$ charge-transfer configuration (d^5L^{-1}; L = ligand), as revealed by photoemission and Mössbauer spectroscopy results (12, 16). This mixing of d^4 and d^5L^{-1} configurations presumably suppresses the Jahn–Teller distortion giving nearly regular FeO$_6$ octahedra in both SrFeO$_3$ and Sr$_2$FeO$_4$. On the other hand, isolated Fe(IV) as in SrLaMg$_{0.5}$Fe$_{0.5}$O$_4$ gives rise to elongated FeO$_6$ octahedra that has been attributed to the high-spin $t_{2g}^3 d_{z^2}^1$ electronic configuration (18).

For small values of x in the series La$_{2-2x}$Sr$_{2x}$Cu$_{1-x}$Fe$_x$O$_4$ investigated here, if we assume that Fe exists as Fe(IV), it would substitute at the Cu(II)

sites of highly distorted (axially elongated: Cu–O bond lengths 4×1.9037 Å; 2×2.424 Å (11)) CuO$_6$ octahedra of the La$_2$CuO$_4$ structure. Accordingly, the most probable configuration of Fe(IV) in this composition range would be $t_{2g}^3 d_{z^2}^1$. The decrease of the a parameter (while the c parameter remains unchanged) could be understood in terms of this electronic configuration. Both the smaller radius of Fe(IV) (as compared to that of Cu(II) (radius of Fe(IV): 0.55 Å (18); radius of Cu(II): 0.73 Å (19)) and the absence of electrons in the $d_{x^2-y^2}$ orbital would ensure highly covalent Fe–O bonds in the xy-plane resulting a contraction of equatorial Fe–O bond lengths, while maintaining the axial Fe–O bond lengths. Concomitant with the change of lattice parameters, we find a decrease in electrical resistivity and a change-over to metallic behavior in the La$_{2-2x}$Sr$_{2x}$Cu$_{1-x}$Fe$_x$O$_4$ system for $x \leq 0.15$, which signal a highly covalent Cu(II)–O–Fe(IV) interaction that delocalizes the charge carriers. This itinerancy of charge carriers implies that there is no correlation energy associated with electron transfer from Cu to Fe and vice versa. Accordingly, the energy involved for the charge-transfer

$$\text{Cu(II)–O–Fe(IV)} \leftrightarrow \text{Cu(III)–O–Fe(III)}$$
$$t_{2g}^6 d_{z^2}^2 d_{x^2-y^2}^1 + t_{2g}^3 d_{z^2}^1 d_{x^2-y^2}^0 \leftrightarrow t_{2g}^6 d_{z^2}^2 d_{x^2-y^2}^0 + t_{2g}^3 d_{z^2}^1 d_{x^2-y^2}^1$$

$$[1]$$
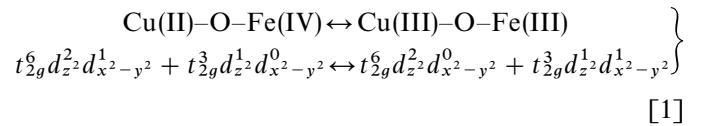
would be nearly zero. This situation would correspond to a valence degeneracy between Cu(II) + Fe(IV) and Cu(III) + Fe(III). Valence degeneracy that results in metallic and ferrimagnetic properties has been known in the perovskite oxide, Ba$_2$FeReO$_6$, wherein the valence states of Fe(II) + Re(VI) are considered degenerate with Fe(III) + Re(V) (7).
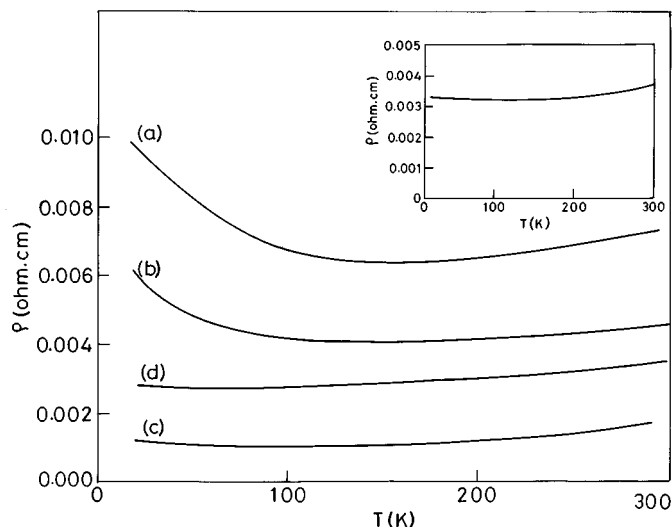
FIG. 8. Plots of resistivity (ρ) versus temperature (T) for $La_{(1.80-y)}Sr_{(0.20+y)}Cu_{0.90}Fe_{0.10}O_4$ for (a) $y = 0.00$, (b) $y = 0.10$, (c) $y = 0.20$, and (d) $y = 0.30$. Inset shows the corresponding data for $La_{1.60}Sr_{0.40}Cu_{0.85}Fe_{0.15}O_4$.

The variation of lattice parameters and the change-over to insulating behavior of $La_{2-2x}Sr_{2x}Cu_{1-x}Fe_xO_4$ for $x > 0.15$ is difficult to rationalize on the basis of the limited experimental data available. One possibility is that for $x > 0.15$, the degenerate valence states represented by [1] shifts toward the right, stabilizing Cu(III) and Fe(III). The increase of a, the decrease of c and the consequent overall decrease of c/a in the system (Fig. 4) together with the insulating behavior are consistent with Cu(III) + Fe(III) valence states, both of which do not support a Jahn–Teller distortion.
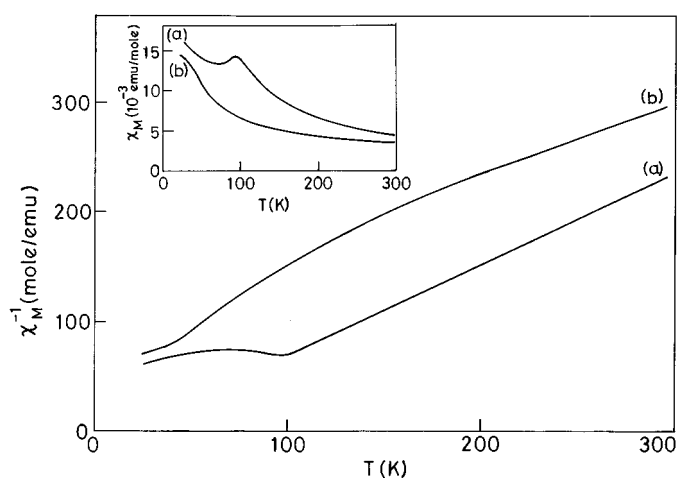
FIG. 9. Plots of inverse molar magnetic susceptibility (χ_M^{-1}) versus temperature (T) for (a) $LaSrCu_{0.50}Mn_{0.50}O_4$, and (b) $LaSrCu_{0.50}Fe_{0.50}O_{4-y}$. Inset shows the corresponding χ_M versus T plots.

We have investigated the effect of hole doping in $La_{1.80}Sr_{0.20}Cu_{0.90}Fe_{0.10}O_4$ and $La_{1.70}Sr_{0.30}Cu_{0.85}Fe_{0.15}O_4$ by substitution of additional Sr^{2+} for La^{3+} that gives $La_{(1.80-y)}Sr_{(0.20+y)}Cu_{0.90}Fe_{0.10}O_4$ and $La_{(1.70-y)}Sr_{(0.30+y)}Cu_{0.85}Fe_{0.15}O_4$ for $y = 0.1$, 0.2, and 0.3. From the resistivity plots (Fig. 8), we see that this doping renders the samples metallic but not superconducting. Obviously, the presence of Fe(IV) (containing unpaired d electrons) at the Cu(II/III) sites of CuO_2 sheets in the La_2CuO_4 structure is detrimental to the formation of superconducting electron pairs.

We have investigated the magnetic susceptibility of $LaSrCu_{0.5}Mn_{0.5}O_4$ and $LaSrCu_{0.5}Fe_{0.5}O_{4-y}$ ($y \sim 0.1$) in an attempt to probe the nature of magnetic interactions in these systems. From the χ_M^{-1} versus T plots (Fig. 9), we see that the susceptibility behavior of the Mn compound at $T > 120$ K is Curie–Weiss-like, the experimental C_M value of 1.18 is comparable to the calculated value of 1.125 assuming Cu(II): $3d^9$ and Mn(IV): $3d^3$ configurations. Similarly, the experimental C_M value of 1.58 for the Fe compound is closer to the C_M value calculated for Cu(II) + Fe(IV) (1.68) than the value calculated for Cu(III) + Fe(III) (2.69) configurations.

The low-temperature magnetic susceptibility behavior of these oxides is different. The Mn oxide shows a broad antiferromagnetic cusp in the χ_M versus T plot (Fig. 9) at $T \sim 95$ K, while the corresponding iron oxide shows a slight enhancement of the susceptibility at $T < 60$ K. The magnetic behavior of the Mn oxide, $LaSrCu_{0.5}Mn_{0.5}O_4$, is surprising at first sight, because the corresponding three-dimensional perovskite La_2CuMnO_6 is known to be ferromagnetic due to a positive $180°$ Cu(II)–O–Mn(IV) interaction (20). Presumably, the antiferromagnetic Cu(II)–O–Cu(II) and Mn(IV)–O–Mn(IV) interactions dominate over the ferromagnetic Cu(II)–O–Mn(IV) interaction because of a random distribution of Cu(II) and Mn(IV) in the layered oxide. An explanation for the low-temperature magnetic behavior of $LaSrCu_{0.5}Fe_{0.5}O_{4-y}$ is not straightforward in view of the presence of an oxygen deficiency in the sample; the oxygen deficiency would introduce mixed-valent states for both copper and iron.

CONCLUSION

In summary, we have shown that it is possible to synthesize new series of K_2NiF_4-like oxides of the general formula, $La_{2-2x}Sr_{2x}Cu_{1-x}^{II}M_x^{IV}O_4$, for $M^{IV} = $ Ti, Mn, Fe, or Ru by the coupled substitution of 2Sr + M^{IV} for 2La + Cu^{II} in the La_2CuO_4 structure. For $M = $ Mn and Fe, the composition range extends $0 < x < 1.00$, while for Ru, it is $0 < x \leq 0.50$ and for Ti, only the $x = 0.50$ member could be prepared. While the $M = $ Ti, Mn, and Ru members are insulating, the $M = $ Fe members for $x \leq 0.15$ are metallic showing a broad metal–semiconductor transition at $T < 100$ K. For $x > 0.20$, members of the $M = $ Fe series show a semiconducting

behavior. The results suggest that the Cu(II)–O–M(IV) interactions are insulating for M = Ti, Mn, and Ru, while the Cu(II)–O–Fe(IV) interaction is itinerant for $x < 0.15$.

REFERENCES

1. J. G. Bednorz and K. A. Müller, *Z. Phys. B* **64,** 189 (1986).
2. J. B. Torrance, Y. Tokura, A. I. Nazzal, A. Bezinge, T. C. Huang, and S. S. P. Parkin, *Phys. Rev. Lett.* **61,** 1127 (1988) and references therein.
3. J. F. Bringley, S. S. Trail, and B. A. Scott, *J. Solid State Chem.* **86,** 310 (1990).
4. T. Hasegawa, K. Kishio, M. Aoki, N. Ooba, K. Kitazawa, K. Fueki, S. Uchida, and S. Tanaka, *Jpn. J. Appl. Phys.* **26,** L337 (1987).
5. M. T. Anderson, K. B. Greenwood, G. A. Taylor, and K. R. Poeppelmeier, *Prog. Solid State Chem.* **22,** 197 (1993).
6. M. T. Anderson and K. R. Poeppelmeier, *Chem. Mater.* **3,** 476 (1991).
7. A. W. Sleight and J. F. Weiher, *J. Phys. Chem. Solids* **33,** 679 (1972).
8. T. Nakagawa, *J. Phys. Soc. Jpn.* **24,** 806 (1968).
9. D. C. Harris and T. A. Hewston, *J. Solid State Chem.* **69,** 182 (1987).
10. W. Lasocha and K. Lewinski, *J. Appl. Cryst.* **27,** 437 (1994).
11. K. Yvon and M. François, *Z. Phys. B* **76,** 413 (1989).
12. P. Adler, *J. Solid State Chem.* **108,** 275 (1994).
13. C. J. O'Connor, *Prog. Inorg. Chem.* **29,** 203 (1982).
14. P. Gómez-Romero, M. R. Palacin, N. Casañ, A. Fuertes, and B. Martinez, *Solid State Ionics* **63–65,** 603 (1993).
15. M. R. Palacin, A. Fuertes, N. Casañ-Pastor, and P. Gómez-Romero, *J. Solid State Chem.* **119,** 224 (1995).
16. A. E. Bocquet, A. Fujimori, T. Mizokawa, T. Saitoh, H. Namatame, S. Suga, N. Kimizuka, Y. Takeda, and M. Takano, *Phys. Rev. B* **45,** 1561 (1992).
17. H. Adachi and M. Takano, *J. Solid State Chem.* **93,** 556 (1991).
18. G. Demazeau, Z. Li-Ming, L. Fournes, M. Pouchard, and P. Hagenmuller, *J. Solid State Chem.* **72,** 31 (1988).
19. R. D. Shannon, *Acta Cryst. A* **32,** 751 (1976).
20. G. Blasse, *J. Phys. Chem. Solids* **26,** 1969 (1965).